EPJ Plus

EPJ.org
your physics journal

Eur. Phys. J. Plus (2018) **133**: 354 DOI 10.1140/epjp/i2018-12168-9

A novel parametrically controlled multi-scroll chaotic attractor along with electronic circuit design

Karthikeyan Rajagopal et al.

Società Italiana di Fisica

Springer

Eur. Phys. J. Plus (2018) **133**: 354
DOI 10.1140/epjp/i2018-12168-9

THE EUROPEAN PHYSICAL JOURNAL PLUS

Regular Article

A novel parametrically controlled multi-scroll chaotic attractor along with electronic circuit design

Karthikeyan Rajagopal[1,a], Serdar Çiçek[2], Peiman Naseradinmousavi[3], Abdul Jalil M. Khalaf[4], Sajad Jafari[5], and Anitha Karthikeyan[1]

[1] Center for Nonlinear Dynamics, College of Engineering, Defense University, Debre Zeyit, Ethiopia
[2] Department of Electronic and Automation, Vocational School of Hacıbektaş, Nevşehir Hacı Bektaş Veli University, 50800 Hacıbektaş, Nevşehir, Turkey
[3] Dynamic Systems and Control Lab., Department of Mechanical Engineering, San Diego State University, San Diego, CA, USA
[4] Department of Mathematics, Faculty of Computer Science and Mathematics, University of Kufa, Najaf, Iraq
[5] Department of Bio-medical engineering, Amirkabir University of Technology, Tehran, Iran

Received: 7 May 2018 / Revised: 24 July 2018
Published online: 6 September 2018

Abstract. We propose a novel multi-scroll chaotic system captured through the Chua's circuit. The novelty of our proposed multi-scroll system roots on the number of scrolls to be controlled by the parameters instead of changing the discontinuous functions repeatedly reported in the literature. We thoroughly investigate dynamical characteristics of the system using powerful tools of the nonlinear dynamic analysis including finite-time local Lyapunov exponents and bifurcation diagram. The practical feasibility of the proposed multi-scroll system is revealed through its electronic realization with off-the-shelf components.

1 Introduction

The studies on chaotic systems have received considerable attention due to their broad applications from fluid flow network to circuit design [1]. Among those chaotic systems, those with multi-scroll attractors are important since they can be utilized in many engineering applications [2–11]. Many efforts were carried out, within the last two decades, to address such multi-scroll attractors [2–6] and their applications in secure communications, circuit design, FPGA implementation, information processing, and encryption [7–11]. Chua and Komuro proposed a two-scroll attractor in [12]. Madan [13] carried out a comprehensive analysis for the properties and modifications of Chua's circuit, which led to new configurations to create various complex multi-scroll chaotic attractors using simple circuits. Suykens and Vandewalle [14] proposed a class of multi-scroll attractors with a single set of mathematical functions.

Note that the multi-scroll attractors are typically obtained through injecting several equilibria into a dissipative system, such that scrolls are generated around each fixed-point. However, there are known multi-scroll attractors which are not formed by unstable manifolds of unstable equilibria [13, 15, 16]. They usually belong to the category of systems with hidden attractors [17–21].

Barajas-Ramirez [16] presented a simple strategy to design multi-scroll attractors with desirable equilibrium points' locations in addition to revealing the transitions expected in the global dynamics. In addition to piecewise linear functions [22, 23], there are some efforts focused on saturated [24], trigonometric, absolute value, polynomial, hyperbolic [25], modulation, sign, and nonlinear hysteresis functions [26]. Lu and Chen [27] studied different design methodologies to generate multi-scroll attractors and also discussed their potential applications.

All these research efforts revealed function-dependent multi-scroll systems which, as expected, need individual functions to generate multiple scrolls motivating us to ask the following critical questions: 1) Why should the multi-scroll attractor be function-dependent? and 2) Why should not be parameter-dependent? Motivated by these questions, we modify Chua's circuit and, to the best of our knowledge, propose the first parameter-controlled multi-scroll attractor.

[a] e-mail: rkarthiekeyan@gmail.com

Table 1. Functions for multiscroll generation.

S.No.	Function type for multiscroll	Reference
1	piecewise linear function	[22,23]
2	saturation function	[24]
3	trigonometric function	[25]
4	polynomial function	[25]
5	hyperbolic function	[25]
6	hysteresis function	[26]
7	signum function	[51]
8	sawtooth function	[30]
9	fixed function with variable parameter	this paper

Some of the function-dependent multi-scroll attractors are compared against the one proposed in this paper as in table 1.

2 Parametrically controlled multi-scroll chaotic attractor (PCMCA)

The classical Chua's system [12] is described by the following state equations:

$$\begin{aligned}\dot{x} &= \alpha(y - x - f(x)),\\ \dot{y} &= x - y + z,\\ \dot{z} &= -\beta y,\end{aligned} \tag{1}$$

where the nonlinear function $f(x)$ is defined as

$$f(x) = \begin{cases} bx + a - b & \text{for } x \geq 1 \\ ax & \text{for } -1 \leq x \leq 1 \\ bx - a + b & \text{for } x \leq -1 \end{cases} \tag{2}$$

This system can generate hidden one-scroll and two-scroll attractors. Chua's circuit generates a two-scroll attractor [28, 29], *e.g.* for $\alpha = 9$, $\beta = \frac{100}{7}$, $a = -1.14$, and $b = -0.7$. We here formulate a multi-scroll attractor from Chua's system (1) by replacing the piecewise linear function, as shown in eq. (3), and also introducing a control parameter c through the state of x in eq. (1). The proposed system becomes as in eq. (4).

$$f(x) = \mathrm{sgn}(x) + \mathrm{sgn}(x + b) + \mathrm{sgn}(x - b) + \mathrm{sgn}(x + 2b) + \mathrm{sgn}(x - 2b), \tag{3}$$

$$\begin{aligned}\dot{x} &= g(y - ax + f(x)) - c,\\ \dot{y} &= x - y + z,\\ \dot{z} &= -dy.\end{aligned} \tag{4}$$

Note that there are many studies focused on multi-scroll attractors formulated by modifying Chua's circuit [30–32], but all employ multiple piecewise linear functions [7,27,33–38]. The novelty of our proposed multi-scroll system roots on the number of scrolls to be controlled by the parameters instead of changing the piecewise linear function. The proposed system is expectedly simple considering the number of terms with respect to the other similar types of multi-scroll systems, which have at least five scrolls; the number of functions required to generate our multi-scroll attractor is one. Therefore, we introduce a new chaotic system based on one of the criteria described in [39].

Table 2 presents a variety of parameters generating different multi-scroll attractors. One may examine other combinations of the parameters which, potentially, lead to such multi-scroll attractors although the maximum scroll may not exceed six due to a restriction for the available thresholds in $f(x)$, which is five.

For the initial conditions $[0.1, 0, 0.1]$ and parameters' values listed in table 1, the phase portraits are shown in figs. 1(a)–(e).

Table 2. The different cases for the system (4).

Multi-scroll attractor	Parameters					Figures
	a	b	g	d	c	
two-scroll	0.3	7	9	15	2.5	1a
three-scroll	0.3	7	9	15	1.5	1b
four-scroll	0.3	7	9	15	1	1c
five-scroll	0.3	7	10	12.5	0.4	1d
six-scroll	0.3	7	10	12	0	1e

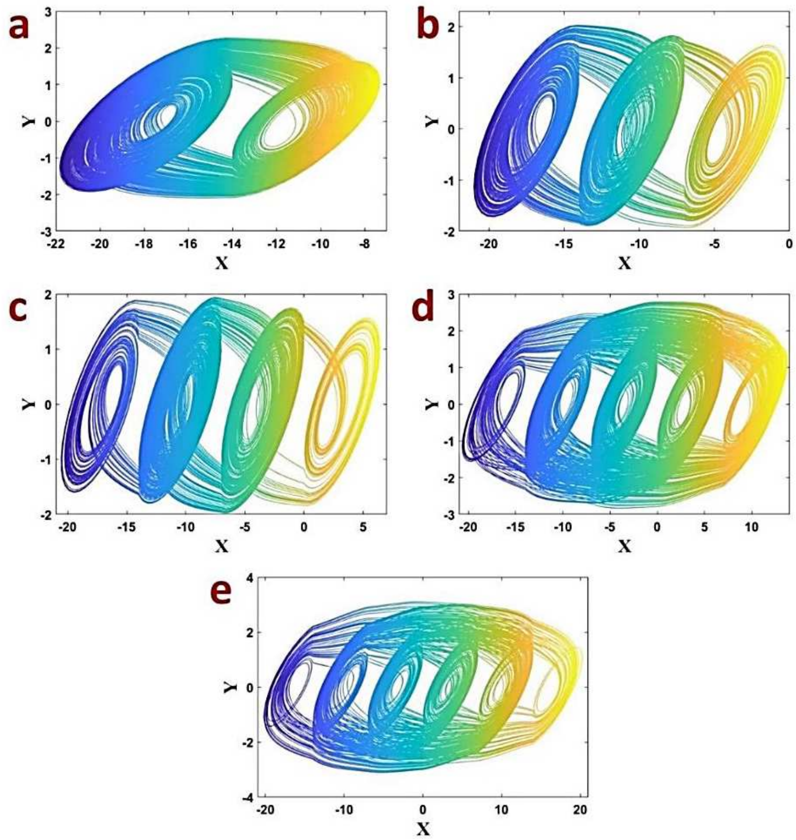

Fig. 1. The 2D (X-Y plane) phase portraits of the PCMCA.

3 Dynamical properties of the PCMCA

The finite-time Lyapunov Exponents (LEs) of the PCMCA are calculated using Wolf's algorithm [40] for 100000s and the initial conditions given as $[0.1, 0, 0.1]$. It is important to be careful about the numerical calculation of Lyapunov exponents, since improper use of usual methods may cause some issues [41–44]. To calculate the LEs, the signum function is replaced with $\tanh(a_1 x)$ to avoid numerical singularities expected. Using higher values of a_1 yields a more accurate representation of the signum function, shown in fig. 2(a), although it will potentially lead to cumbersome complexities for real-time implementations in both analog and digital circuits. Therefore, we select $a_1 = 100$ for the calculation of LEs, whereas a negligible difference (< 0.0006) is noted using $a_1 = 100$ and $a_1 = 500$. Shown in fig. 2(b) are the finite-time local Lyapunov exponents of the mentioned system calculated for various values of a_1. The LEs and the corresponding Kaplan-Yorke dimension (D_{KY}), for the multi-scroll systems, are given in table 2.

The dynamic behavior of the PCMCA system is visualized by plotting its bifurcation diagram *vs.* c, as the control parameter, and using the other parameters listed in table 3; for the two-scroll system. Shown in fig. 3 are the bifurcation diagrams of the PCMCA system. The blue dots indicate the bifurcation derived using forward continuation (by increasing the control parameter with reinitializing the initial conditions to the end values of state variables in every iteration), while the red dots stand for the bifurcation captured through backward continuation (by decreasing the control parameter with reinitializing the initial conditions to the end values of state variables in every iteration). Note

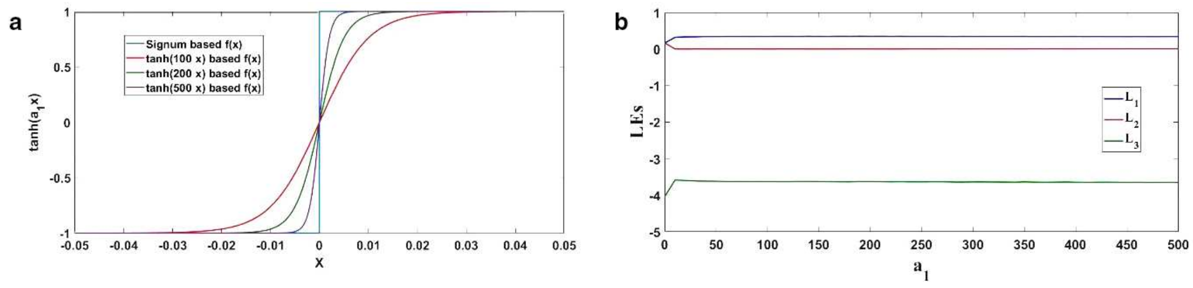

Fig. 2. (a): The signum function and $\tanh(a_1 x)$; (b): The finite-time local Lyapunov exponents of the two-scroll system calculated for various values of a_1.

Table 3. The finite-time local Lyapunov exponents of the PCMCA system.

Multi-scroll attractor	LEs	D_{KY}
two-scroll	0.347, 0, −3.625	2.095
three-scroll	0.347, 0, −3.623	2.095
four-scroll	0.348, 0, −3.599	2.096
five-scroll	0.726, 0, −3.584	2.2
six-scroll	0.754, 0, −3.466	2.217

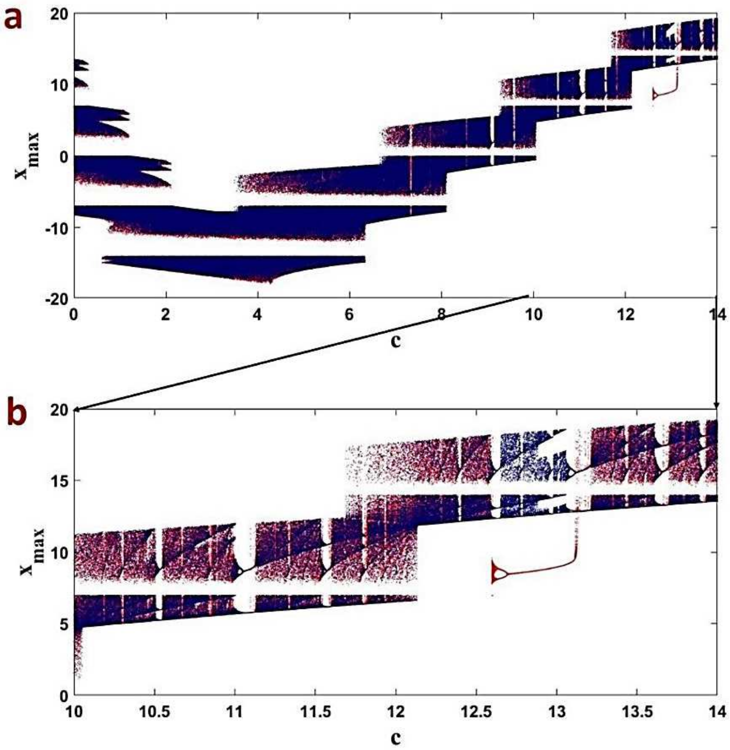

Fig. 3. (a) The bifurcation diagram of the PCMCA system *vs.* the control parameter with the range of $0 < c < 14$ for the two-scroll case; (b) the diagram within $12.6 < c < 13.2$.

that we plotted local maxima of the state variable x. Figure 3(a) presents the bifurcation diagram *vs.* the control parameter with the range of $0 < c < 14$. Figure 3(b) shows the diagram for the range of $10 < c < 14$ revealing the coexistence of a limit cycle with a chaotic attractor within $12.6 < c < 13.2$. Also, it is of a great interest to observe the coexistence of a single-scroll chaotic attractor (red) and a period-1 limit cycle (blue) for initial conditions $[-18, 5, 34]$ and $[-0.1, 0, 0.1]$, respectively, and $c = 12.83$ as shown in fig. 4. Note that such a multistability property makes our proposed system much more interesting to be utilized, since the multistable systems, with coexisting attractors, are highly important in nonlinear dynamics [45–50].

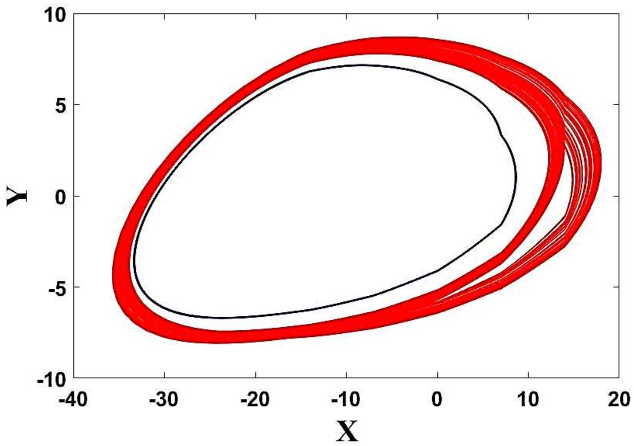

Fig. 4. The coexistence of a single-scroll chaotic attractor (red) and a period-1 limit cycle (blue) for initial conditions $[-18, 5, 34]$ and $[-0.1, 0, 0.1]$, respectively, and $c = 12.83$.

4 Electronic circuit design of the four-scroll PCMCA system for engineering applications

We here design the electronic circuit, based on OP-AMP (Operational Amplifier) devices of the four-scroll parametrically controlled multi-scroll chaotic attractor (PCMCA), to be employed in broad engineering applications. We utilize OrCAD PSpice program in designing the electronic circuit. It should be noted that while PSpice software is based on actual circuit components, it still suffers from the discretization and its usage can lead to wrong conclusions especially for hidden attractors [21]. The values of the state variables x and z of the four-scroll PCMCA system vary between $-25\,\mathrm{V}$ to $30\,\mathrm{V}$. Note that the maximum supply voltage of the OP-AMP device used in the circuit is $\pm 18\,\mathrm{V_{dc}}$. Therefore, the values and initial conditions of state variables x and z are scaled by 5 as in eq. (5). Also, the system and piecewise linear function (f) scaled by 5 are represented in eq. (6). We rename the state variables of the scaled system as X, Y, and Z. The initial conditions of the scaled system are $X_0 = 0.02$, $Y_0 = 0.02$, and $Z_0 = 0.02$.

$$X = \frac{x}{5} \Rightarrow \dot{X} = \frac{\dot{x}}{5}\,, \qquad Z = \frac{z}{5} \Rightarrow \dot{Z} = \frac{\dot{z}}{5}\,, \tag{5}$$

$$\begin{aligned} \dot{X} &= -1.8Y + 2.7X - 1.8f + 0.2, \\ \dot{Y} &= -5X + Y - 5Z, \\ \dot{Z} &= 3Y, \\ f &= \mathrm{sgn}(x) + \mathrm{sgn}(x+1.4) + \mathrm{sgn}(x-1.4) + \mathrm{sgn}(x+2.8) + \mathrm{sgn}(x-2.8). \end{aligned} \tag{6}$$

Figure 5 presents a schematic of the electronic circuit designed. The electronic circuit has the following analog devices: 1) six TL084 ICs, 2) three capacitors, and 3) forty-eight resistors. The supply voltage of the electronic circuit is $\pm 12\,\mathrm{V_{dc}}$. The values for the electronic components of the circuit (fig. 5) are given in table 4.

The state-space equations of the electronic circuit are as

$$\begin{aligned} \dot{X} &= -\frac{1.8}{R_{38}C_1}Y + \frac{1}{R_{37}C_1}X - \frac{1.8}{R_{39}C_1}f + \frac{0.2}{R_{40}C_1}\,, \\ \dot{Y} &= -\frac{1}{R_{46}C_2}X + \frac{1}{R_{45}C_2}Y - \frac{1}{R_{47}C_2}Z, \\ \dot{Z} &= \frac{1}{R_{48}C_3}Y. \end{aligned} \tag{7}$$

Shown in fig. 6 are the state variables (X, Y, Z) of the electronic circuit designed for the scaled four-scroll PCMCA system (6). The state variables vary as $-5\,\mathrm{V} < X < 3\,\mathrm{V}$, $-2\,\mathrm{V} < Y < 2\,\mathrm{V}$, and $-3\,\mathrm{V} < Z < 6\,\mathrm{V}$. Therefore, it is straightforward to conclude that the scaled system (6) is practically applicable in the field of electronic circuits.

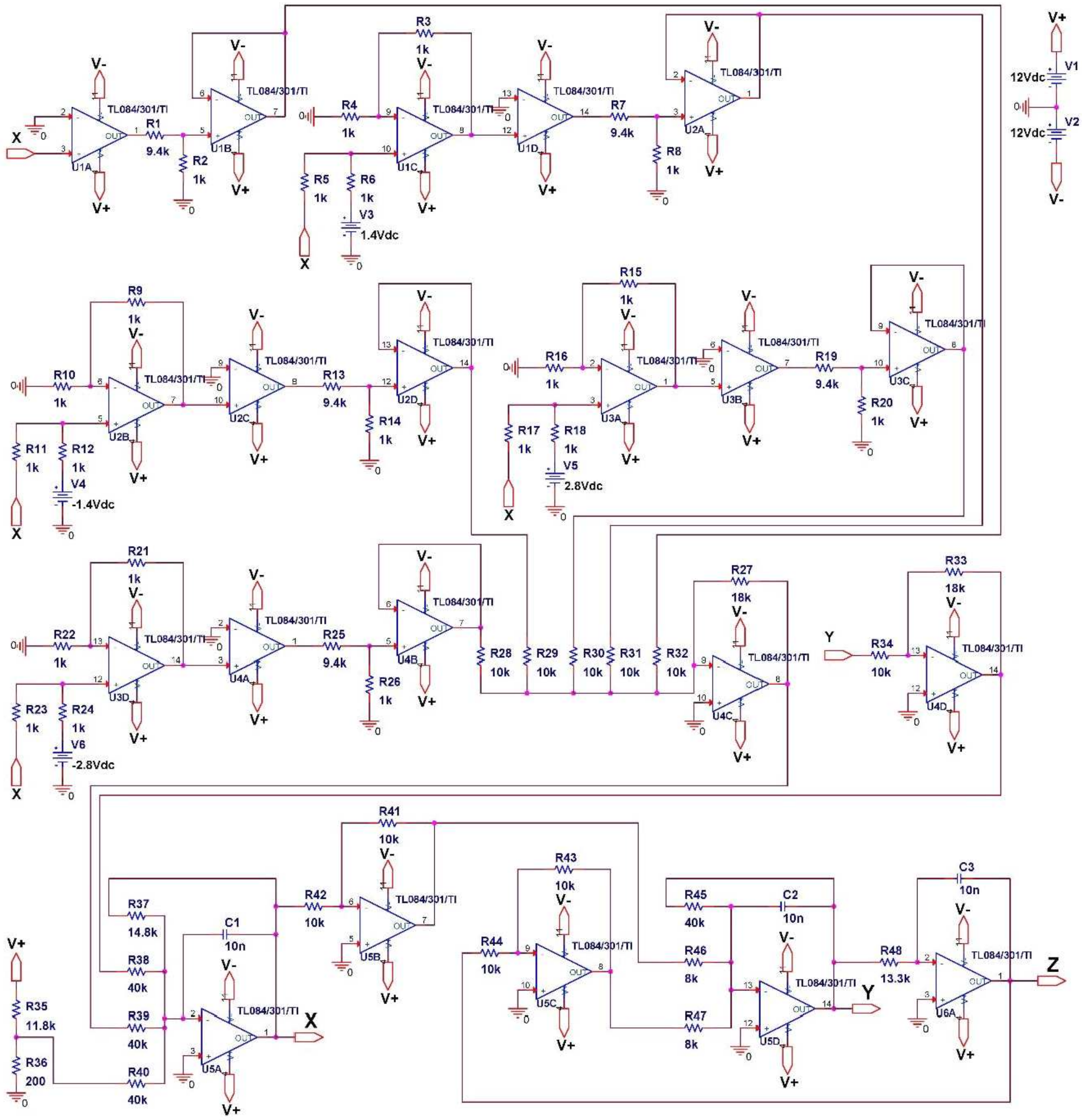

Fig. 5. A schematic for the electronic circuit of the four-scroll PCMCA system.

Table 4. The values for the electronic components of the circuit.

Device name	Value
U1, U2, U3, U4, U5, U6	TL084 IC
C1, C2, C3	10 nF
R1, R7, R13, R19, R25	9.4 k
R2, R3, R4, R5, R6, R8, R9, R10, R11, R12, R14, R15, R16, R17, R18, R20, R21, R22, R230, R24, R26	1 kΩ
R27, R33	18 kΩ
R28, R29, R30, R31, R32, R34, R41, R42, R43, R44	10 kΩ
R35	11.8 kΩ
R36	200 Ω
R37	14.8 kΩ
R38, R39, R40, R45	40 kΩ
R46, R47	8 kΩ
R48	13.3 kΩ

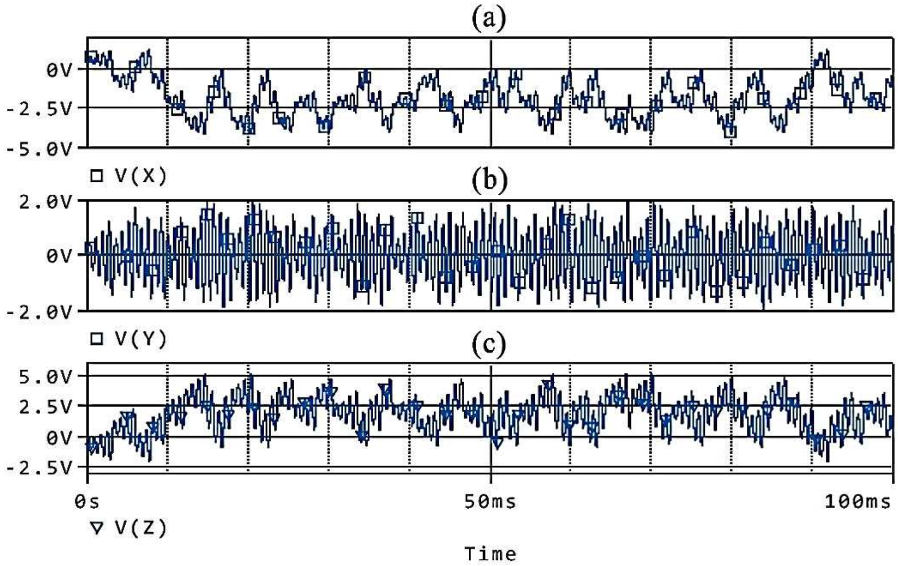

Fig. 6. The output signals of the electronic circuit designed as in fig. 5: (a) X; (b) Y; (c) Z.

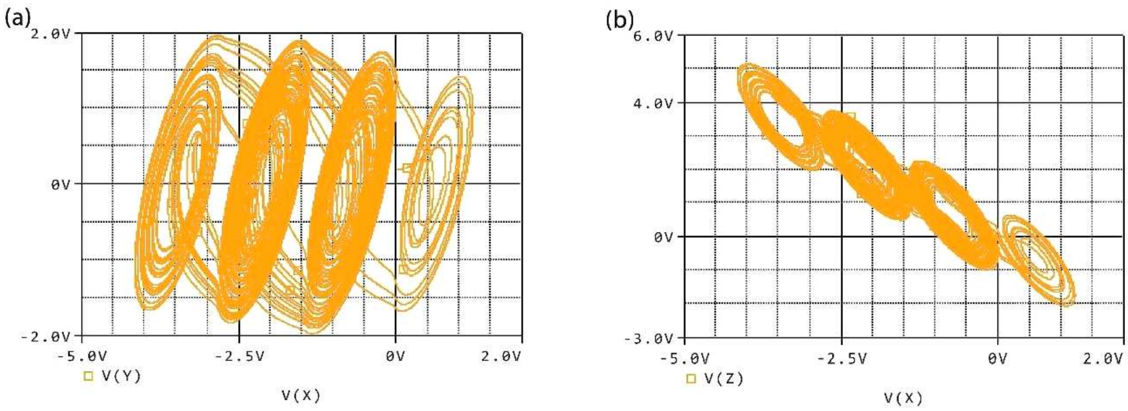

Fig. 7. The phase portraits of the electronic circuit are designed as in fig. 5.

Figure 7 presents the phase portraits of the electronic circuit. It is worth mentioning that the phase portrait of the four-scroll PCMCA system (fig. 1(c)) is the same as the phase portrait of the electronic circuit designed (fig. 7(a)). Subsequently, we can easily conclude that, based the electronic circuit designed, the PCMCA system is applicable in broad engineering problems.

5 Conclusions

In this paper, we proposed a novel multi-scroll chaotic system whose scrolls were parametrically controlled instead of being function-dependent. The significant advantage of such a system design was visualized through its real-time implementation in hardware, whereas a single function expectedly requires less resources to be implemented. Also, the scrolls were controlled by only changing the parameters, which here was achieved through varying the discrete components. The proposed system revealed rich dynamical behaviors, which we thoroughly investigated employing the powerful tools of finite-tine local Lyapunov exponents and bifurcation diagram. We captured the coexistence of a limit cycle with a chaotic attractor, in addition to the coexistence of a single-scroll chaotic attractor and a period-1 limit cycle, subject to some initial conditions and crucial values of the control parameter c. This led us to the multistability aspect of our proposed system, which is counted as a highly important property for broad nonlinear dynamical systems. Finally, we realized the system proposed as electronic circuits using off-the-shelf components and then presented simulation results to evaluate our novel circuit design. Such multiscroll chaotic systems which could produce different scrolls for just a simple change in a resistance or capacitance (in analog circuits) can be very useful in chaos-based communication systems.

References

1. J.C. Sprott, *Elegant Chaos: Algebraically Simple Chaotic Flows* (World Scientific, 2010).
2. R. Trejo-Guerra *et al.*, Commun. Nonlinear Sci. Numer. Simul. **17**, 4328 (2012).
3. C. Li, S. Yu, X. Luo, Int. J. Bifurc. Chaos **23**, 1350170 (2013).
4. L.G. de la Fraga, E. Tlelo-Cuautle, Nonlinear Dyn. **76**, 1503 (2014).
5. E. Tlelo-Cuautle *et al.*, Nonlinear Dyn. **85**, 2143 (2016).
6. J. Ma *et al.*, PLoS ONE **13**, e0191120 (2018).
7. J. Ma *et al.*, Nonlinear Dyn. **76**, 1951 (2014).
8. M. García-Martínez *et al.*, Appl. Math. Comput. **270**, 413 (2015).
9. E. Tlelo-Cuautle *et al.*, Commun. Nonlinear Sci. Numer. Simul. **27**, 66 (2015).
10. F. Li, J. Ma, PLoS ONE **11**, e0154282 (2016).
11. A.D. Pano-Azucena *et al.*, Nonlinear Dyn. **87**, 2203 (2017).
12. T. Matsumoto, L. Chua, M. Komuro, IEEE Trans. Circ. Syst. **32**, 797 (1985).
13. N. Kuznetsov *et al.*, Nonlinear Dyn. **92**, 267 (2018).
14. J.A. Suykens, J. Vandewalle, IEEE Trans. Circ. Syst. I **40**, 861 (1993).
15. G.A. Leonov, N.V. Kuznetsov, T.N. Mokaev, Eur. Phys. J. ST **224**, 1421 (2015).
16. G.A. Leonov, N.V. Kuznetsov, Int. J. Bifurc. Chaos **23**, 1330002 (2013).
17. G. Leonov, N. Kuznetsov, V. Vagaitsev, Physica D **241**, 1482 (2012).
18. G. Leonov *et al.*, Nonlinear Dyn. **77**, 277 (2014).
19. M.-F. Danca, N. Kuznetsov, Chaos, Solitons Fractals **103**, 144 (2017).
20. M.-F. Danca, N. Kuznetsov, G. Chen, Nonlinear Dyn. **88**, 791 (2017).
21. N. Kuznetsov *et al.*, Commun. Nonlinear Sci. Numer. Simul. **51**, 39 (2017).
22. E. Campos-Cantón *et al.*, Rev. Mex. Fís. **54**, 411 (2008).
23. E. Campos-Cantón *et al.*, Chaos **20**, 013116 (2010).
24. J. Lu *et al.*, IEEE Trans. Circ. Syst. I **51**, 2476 (2004).
25. F. Xu, P. Yu, J. Math. Anal. Appl. **362**, 252 (2010).
26. J. Lü *et al.*, Automatica **40**, 1677 (2004).
27. J. Lü, G. Chen, Int. J. Bifurc. Chaos **16**, 775 (2006).
28. N.V. Stankevich *et al.*, Int. J. Bifurc. Chaos **27**, 1730038 (2017).
29. G. Leonov, N. Kuznetsov, V. Vagaitsev, Phys. Lett. A **375**, 2230 (2011).
30. F.-Q. Wang, C.-X. Liu, Int. J. Mod. Phys. B **22**, 2399 (2008).
31. D. Chen *et al.*, Int. J. Circ. Theory Appl. **42**, 407 (2014).
32. L. Gámez-Guzmán *et al.*, Commun. Nonlinear Sci. Numer. Simul. **14**, 2765 (2009).
33. W.K. Tang *et al.*, IEEE Trans. Circ. Syst. I **48**, 1369 (2001).
34. L. Wang, Nonlinear Dyn. **56**, 453 (2009).
35. J. Muñoz-Pacheco *et al.*, Int. J. Electron. **101**, 1559 (2014).
36. T. Zuo *et al.*, IEEE Trans. Circ. Syst. II **61**, 818 (2014).
37. E. Tlelo-Cuautle *et al.*, Commun. Nonlinear Sci. Numer. Simul. **27**, 66 (2015).
38. S. Jafari, V.-T. Pham, T. Kapitaniak, Int. J. Bifurc. Chaos **26**, 1650031 (2016).
39. J.C. Sprott, Int. J. Bifurc. Chaos **21**, 2391 (2011).
40. A. Wolf *et al.*, Physica D **16**, 285 (1985).
41. A. Stefanski, A. Dabrowski, T. Kapitaniak, Chaos, Solitons Fractals **23**, 1651 (2005).
42. G.A. Leonov, N.V. Kuznetsov, Int. J. Bifurc. Chaos **17**, 1079 (2007).
43. N. Kuznetsov, T. Mokaev, P. Vasilyev, Commun. Nonlinear Sci. Numer. Simul. **19**, 1027 (2014).
44. N. Kuznetsov, Phys. Lett. A **380**, 2142 (2016).
45. Q. Lai, S. Chen, Optik **127**, 3000 (2016).
46. Q. Lai, L. Wang, Optik **127**, 5400 (2016).
47. A. Chudzik *et al.*, Int. J. Bifurc. Chaos **21**, 1907 (2011).
48. T. Kapitaniak, G.A. Leonov, Eur. Phys. J. ST **224**, 1405 (2015).
49. H. Bao *et al.*, Commun. Nonlinear Sci. Numer. Simul. **57**, 264 (2018).
50. M. Chen *et al.*, Nonlinear Dyn. **91**, 1395 (2018).
51. Xinzhi Liu, Xuemin Sherman Shen, Hongtao Zhang, Int. J. Bifurc. Chaos **22**, 02 (2012).